ISSN: 2584-0355
DOI: doi.org/10.51219/MCCRJ/Giulio-Fanti/417

URF PUBLISHERS
connect with research world

Medical & Clinical Case Reports Journal

https://urfpublishers.com/journal/case-reports

Vol: 3 & Iss: 4

Review

Shroud of Turin: Reverse Engineering to Reconstruct The Tools That Produced The Scourge Marks

Giulio Fanti*, Matteo Cardin, Vittorio Cinquetti, Marta Romanello, Leonardo Rizzotto, Antonio Rozzi Marin, Luca Simonetti

Department of Industrial Engineering, University of Padua, via Venezia 1, 35131 Padua, Italy

Citation: Fanti G, Cardin M, Cinquetti V, et al. Shroud of Turin: Reverse Engineering to Reconstruct The Tools That Produced The Scourge Marks. *Medi Clin Case Rep J* 2025;3(4):1487-1494. DOI: doi.org/10.51219/MCCRJ/Giulio-Fanti/417

Received: 04 November, 2025; **Accepted:** 02 December, 2025; **Published:** 04 December, 2025

***Corresponding author:** Giulio Fanti, Department of Industrial Engineering, University of Padua, via Venezia 1, 35131 Padua, Italy

A B S T R A C T

The recently released UV photographs of the Turin Shroud (TS or Holy Shroud), now available for scientific analysis, have made it possible to better highlight the scourge wounds. For this reason, previous analyses based on photographs taken in visible light have been updated, increasing the number of bloodstains from 372 to nearly 500. However, considering that many scourge marks are not encoded in the TS because it was not in contact with all parts of the wrapped human body, it can be assumed that the scourge wounds inflicted on Jesus could have numbered 800 or more.

The bloodstains were measured in detail and then categorized into different groups, including: Dumbbell, Scratches and Rod-like blows. Finally, through reverse engineering supported by experimental tests, the three types of whips mentioned, which produced the bloodstains visible on the TS, were reconstructed.

Keywords: Turin Shroud; Bloodstains; Flagrum; Scourge marks, Torture

Introduction

A few studies [1-10], show that the TS is a handmade 3:1 twill linen cloth, 4.4 m long and 1.1 m wide, on which the front and back images of a human body are permanently and mysteriously imprinted [5,6,11,12].

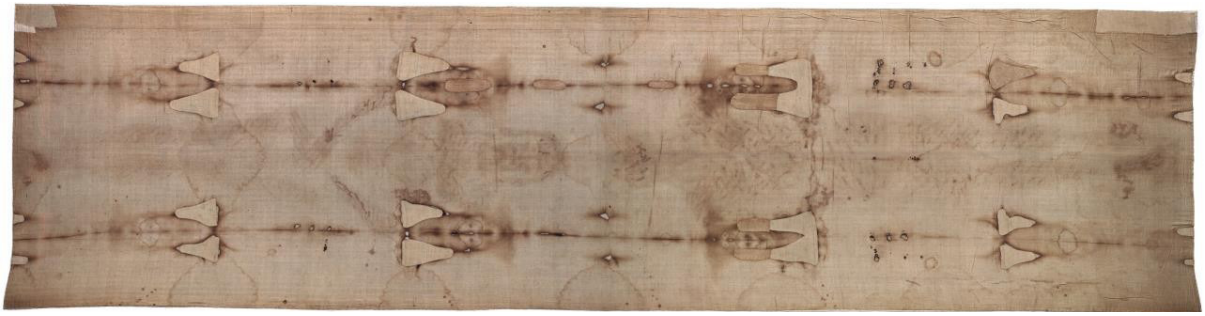

Figure 1: Holy Shroud of Turin photographed by G. Durante in 2000 (Archdiocese of Turin).

According to Pope Julius II [13], who approved the Mass and the Office of the TS in 1506 and declared that it had to be not only venerated but also adored and the subsequent Catholic Christian tradition, the TS is the burial cloth in which the body of Jesus Christ was wrapped before being placed in a tomb in Palestine about 2000 years ago, **(Figure 1)**.

The Catholic Christian Church does not impose any veneration requirements of the TS, even though science has been unable to refute what is reported by tradition.

There are some indications that the TS was in Palestine in the first century A.D. and then taken to Edessa [14,15] (present-day Sanliurfa in Turkey) but other scholars hypothesize different paths for this Relic [16].

Several features found on the facial image on the TS accurately coincide with those found on depictions of Christ on Byzantine coins starting from the VII century A.D. which provides evidence that the TS was seen during the Byzantine Empire [15]. After disappearing during the Sack of Constantinople in 1204, the "Shroud of Christ" then, later, appeared in Europe in 1353 in Lirey in France. In 1532, a fire damaged it at Chambéry in France. In 1578, it was taken to Turin where it has remained until now, apart from some short periods of time when it was hidden during wartime.

In 1988, radiocarbon dating of the TS yielded an erroneous date range of 1260-1390 AD [16]. This result remains a subject of ongoing debate [3,17-22], with multiple studies challenging its reliability due to very probable contamination especially caused by environmental factors.

Recent findings, including the detection of Beta radioactivity and fluorescence in the bloodstains on the TS [1,23-25] further confirm the inaccuracy of the radiocarbon dating results. These discoveries suggest that neutron reactions related to the body image formation may have skewed the radiocarbon measurements.

The presence of selective radioactivity detected in the TS serves as a strong indication that the 1988 radiocarbon dating results are biased by an intense neutron flux that altered the isotopic composition of the linen fibers, leading to a younger apparent radiocarbon age. Such a neutron flux could be easily associated with the Resurrection of Jesus Christ.

Recent studies [23,24] has demonstrated that, from a medical perspective, it is virtually impossible for a medieval artist to have produced the bloodstains observed in correspondence with the double body image on the TS.

These stains, which exhibit distinct morphological variations, can only be coherently explained by considering the TS as having been wrapped around a human body that underwent severe torture and crucifixion in accordance with execution practices of Roman types, as described in the Christian Holy Bible (CHB).

Moreover, specific characteristics of these bloodstains, such as the absence of smearing, further suggest the presence of a phenomenon that remains scientifically unexplained, potentially pointing to a miraculous occurrence.

Recent analyses of blood samples collected from the TS [1,3,4,23-29] have provided novel insights into the physiological state of Jesus Christ during His Passion, crucifixion and entombment described in the CHB. One of the key conclusions emerging from this research is the hypothesis concerning the mode of Christ's departure from the TS following the estimated 30 to 40 hours post-mortem. The study proposes a novel interpretation based on the concept of material transparency, demonstrating that Jesus' body came out of the TS in a way that did not touch the integrity of the cloth.

The first author, analysing the visible-light photographs of the TS taken by Gian Durante in 2000 and 2002, counted 159 scourge wounds on the frontal image and 213 on the dorsal image, for a total of 372 wounds [30]. This number was obviously likely to increase if one considered the imperceptible marks on the photographs and especially considering the fact that the TS was not in contact with all the lateral parts of the wrapped human body.

Since the ultraviolet (UV) photographs of the TS taken by Miller in 1978 [31] have recently been made available to scholars, which, as is well known, better highlight bloodstains, this study attempted to highlight the scourge marks less identifiable on G. Durante's photographs. The number of bloodstains produced by the scourges was then recounted and these marks were grouped into different classes.

It is not easy to find many references to the scourges used in Roman times [32-35] and there have been criticism [36] on the fact that the signs of scourge visible on the TS are truly attributable to historically preserved or known scourges.

Consequently, the reverse engineering method for the classes of scourge wounds more clearly defined was carried out to the TS, comparing the TS marks with those made by appropriate torture tools designed and built.

Identification of Signs of Scourges

The study was conducted using G. Durante's photographs (2002) for their quality and high resolution and V. Miller's ultraviolet (UV) photographs (1978) [31] because blood traces are more evident at that wavelength. The image of the TS was first cropped to evidence the frontal and dorsal image of Jesus Christ and then the size of the square pixels was determined to be 0.192 ± 0.002 mm.

As shown in **(Figure 2)**, the Fast Fourier Transform and its inverse were applied using ImageJ® software to reduce the effect of the linen weave. Subsequently, by analysing the image histogram using Paint Shop Pro® 2023 software and adjusting the gamma values, a result was achieved that better highlighted the scourge wounds.

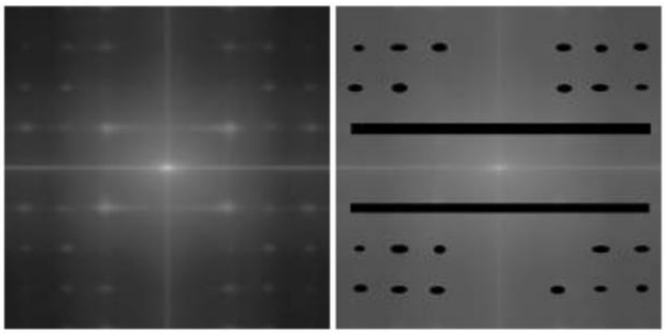

Figure 2: On the left, a contrasted image of the TS linen fabric obtained from the Fourier Transform, highlighting the peaks (brighter areas) of the spatial frequencies of the weave is shown. On the right, we see the same image indicating the black areas added to filter out the weave effect.

Ten distinct categories of scourge marks were first identified and their characteristic dimensions were determined using ImageJ® software, as reported in **(Table 1)**. The table includes representative images for each category.

The initial 10 categories were subsequently consolidated into 6 by merging those with similar characteristics, under the assumption that the same torture instrument could have caused morphologically slightly different wounds depending on the area of the human body that was struck.

Each of the categories described below is associated with a colour, highlighted in **(Figure 3)**. It becomes evident that different pairs of flagellators (perhaps three) most likely acted independently, one after the other, targeting specific areas of the human body.

It should be noted that this analysis perhaps includes in the categories of scourge marks possible marks from lashes Jesus received during the carrying of the cross to Calvary.

Category α: **dumbbell** in red;

Category β: **parallel scratches** in orange;

Category γ: **non-parallel scratches** in green;

Category δ: **rod-like scratches** in light blue;

Category X: **unclassifiable** marks in blue;

Category Y: **possible** marks in pink.

Dumbbell scratches category α

Regarding the dumbbell category, a higher concentration of these marks is observed in the back area of the dorsal image. In the frontal image, however, they are predominantly located on the chest and shins. This distribution was probably intentional, aiming to avoid damaging certain vital organs.

Table 1: Characterization of the 10 categories of scourge marks identified on the TS.

1. Dumbbell α	Size [mm] Diameter D= 12 - 7 Length L= 35 - 18 Width S= 7,3 - 3,8 Example of coordinate: D.D16	6. Non-parallel scratches γ	Size [mm] Length L= 42 – 24 Angle α= 8° - 4° Example of coordinate: D.E29
2. Dumbbell with scratches α	Size [mm] Diameter D= 10 - 7 Length L= 30 - 19 Width S= 12 - 7 Scratches distance G= 5 - 2 Example of coordinate: D.D8	7. Big non-parallel scratches γ	Size [mm] Diameter D= 60 - 33 Angle α= 25° - 4° Example of coordinate: F.D19
3. Single ball α	Size [mm] Diameter D= 10 - 8 Length L= 43 - 25 Width S= 14 - 7 Scratches distance G= 5 - 3 Example of coordinate: D.F24	8. Horizontal whips δ on the arms	Size [mm] Length L= 70 - 38 Width S= 13 – 7 Example of coordinate: F.G11
4. Many parallel scratches β	Size [mm] Length L= 39 - 14 Width S= 15 - 5 Distance G= 6 - 1 Example of coordinate: D.D16	9. Vertical whips δ on the legs	Size [mm] Length L= 166 - 41 Width S= 14 – 7 Example of coordinate: F.F17
5. Two parallel scratches β	Size [mm] Length L= 29 - 21 Width S= 6 - 4 Distance S= 4 - 2 Example of coordinate: D.G5	10. Vertical whips δ on the shoulders	Size [mm] Length L= 30 - 19 Width S= 5 – 3 Example of coordinate: D.B6 NOTE: some of them are out of the body image

The orientation of these marks is predominantly vertical in the upper and lower areas of the body, suggesting the blows were inflicted from top to bottom and vice versa. In the central part of the body, the marks are oriented almost horizontally, in a radial pattern.

The difference in the size of the marks detected between the right and left sides of the body suggests the presence of two different flagellators.

Parallel scratches category β

The **parallel scratches** category shows a higher density of marks on the chest, particularly the right side, while on the legs, both front and back, these marks appear less numerous and more evenly distributed. Again, an asymmetry between the right and left sides of the chest is noticeable, suggesting two different flagellators. The preferential orientation of the scratches suggests they may have been inflicted by at least one left-handed flagellator.

Non-parallel scratches category γ

The **non-parallel scratches** category is found more on the legs; a high-density area of such marks is located on the left calf. In this case as well, the shape of the wounds suggests the presence of a left-handed flagellator.

Rod like blows category δ

Regarding the **rod-like blows** category, these are predominantly distributed on the frontal image, particularly along the arms and quadriceps. In the latter area, the orientation of the marks appears to run from bottom to top and is mirrored on the right and left sides. In the dorsal image, however, a higher density is detected on the back, where the wounds show a radial inclination similar to that observed for the other categories of scourge marks.

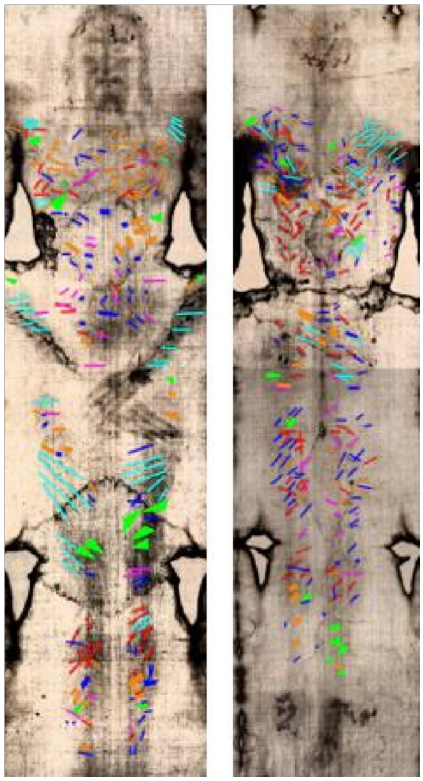

Figure 3: Durante's photograph of the body of Jesus Christ with each type of scourge mark highlighted, each with a specific color: on the left is the frontal image, on the right is the dorsal one.

Unclassifiable scratches category X

Regarding the **Unclassifiable marks** Category, they appear sporadically distributed over the entire body, with a higher concentration on the abdomen. This is perhaps because the position of the arms hindered perfect contact between the body and the cloth, thus compromising the formation of clearer marks that would be easier to classify.

Possible scratches category Y

Regarding the **Possible marks** Category, they have been identified as wounds, but not as definitive scourge marks and are generally located adjacent to those in Category X.

In this study, we define "mark" as a wound produced by an instrument connected to a single cord. A flagrum could have consisted of approximately 3-7 cords, but this is irrelevant in subsequent counting. If the blow completely touched the skin, we have a complete mark, but in some cases, the instrument-skin contact was incomplete and the corresponding marks were classified as Category X.

(Table 2) shows the number of scourge marks identified on both the front and back image for all 6 categories. Considering the total number of scourge marks, the count amounts to 441 marks, with an uncertainty range of +51/-0, to which an additional uncertainty of ±10 is added. This additional uncertainty accounts for the subjectivity involved in identifying the scourge marks.

This number, of course, does not include the wounds that were certainly present on the human body in the lateral areas and on the inner parts of the arms and legs, as these are not visible on the TS because it was not in contact with those parts.

Table 2: Number of scourge marks detected both in the frontal and dorsal image for the 6 categories detected on the TS.

Number of scourge marks detected for each category	Frontal image	Dorsal image	Total
α Dumbell	42	79	121
β Parallel scratches	46	32	78
γ Non-parallel scratches	16	13	29
d Rod like blows	36	31	67
X Unclassifiable	53	93	146
Y Possible marks	24	27	51

Reverse Engineering for the Reconstruction of the Scourges

Given the lack of extensive bibliographic resources concerning the types of scourges used in the first century A.D. [36], an attempt was made to reconstruct the form of the torture instruments used for Jesus through the application of reverse engineering to the morphology of the marks visible on the TS.

Specifically, through a trial-and-error procedure, experimental scourges were reconstructed based on the most well-defined scourge marks visible on the TS, which were considered as reference samples. By comparing the marks caused by these experimental scourges with those on the TS, the design of the experimental scourges was subsequently refined until marks compatible with the reference ones were obtained.

To produce the experimental marks, the scourge prototypes were used on surfaces simulating parts of the human body. These surfaces needed to be sufficiently malleable upon impact from the scourge, yet sufficiently rigid to guarantee a consistency similar to human flesh. Salt-dough, composed of 1 kg of soft

wheat flour, 0.5 kg of water and 0.5 kg of fine salt, was therefore used.

Some tests were also carried out by placing one or two sheets of transparent food-wrap-film over the salt-dough to reduce friction and better simulate human skin. In this case too, the marks produced were similar to the previous ones. Finally, it should be noted that the scourge does not get stuck in the salt dough but bounces back or slides, as might have happened with a human body.

The results obtained for the main categories of marks on the TS, which enabled the construction of the instruments starting from the classification carried out, are presented below.

Type α scourges for the dumbbell marks

The scourge prototypes were designed with reference to instruments that were simple in construction, using materials easily available 2000 years ago and whose purpose was to inflict pain on the condemned without causing sudden death.

It was assumed that the scourge consisted of a handle to which several cords were attached, at the ends of which two lead balls were connected, lead being an inexpensive material, easy to melt (melting point 327 °C) and therefore workable.

The connection of these balls to the cords was considered according to two different hypotheses, see **(Figure 4)**: the first (left in the figure) considers the two balls, separated from each other by an additional element, threaded consecutively onto the cord; the second hypothesis (right in the figure), instead, contemplates the possibility that the two balls were connected perpendicularly to the cord. This second hypothesis was, however, subsequently discarded because the scratches visible on the TS seem parallel to the line connecting the centres of the two balls, whereas this second Type of scourge would leave scratches perpendicular to this connecting line.

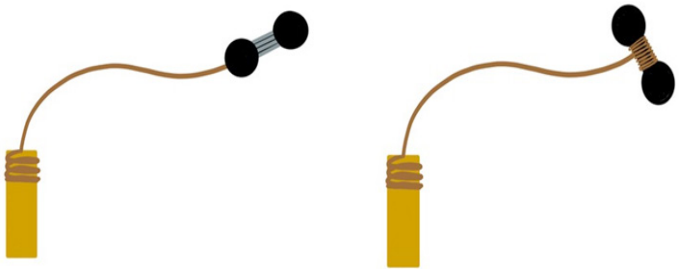

Figure 4: On the left, a model of Type α scourge with two small balls threaded consecutively onto the scourge's cord (the chosen solution). On the right, the cord is perpendicular to the line connecting the centers of the two balls (the discarded solution). A third, sharp body consisting of a grooved lead cylinder was placed between the two balls of the scourge to produce the scratches.

For the scratches present between the two balls, several possibilities were studied, including the presence of a third body between the two balls. After various tests, a scourge was obtained formed by two spherical fishing sinkers, not pierced but partially cut, with a mass of 1.8 g and a diameter of 7 mm, crimped onto the cord.

A lead cylinder, with a mass of 10 g, a length of 16 mm and an average diameter of 5.5 mm, pre-drilled along its axis and grooved on the external surface via irregular cuts, was inserted between the two balls. This cylinder was thus capable of producing scratches similar to those visible on the TS. This experimental scourge produced impressions compatible with those on the TS, both in shape and size, see **Figure 5**.

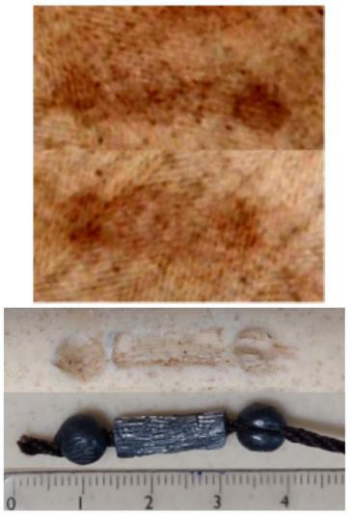

Figure 5: Top: an example of a Type α scourge mark on the TS. Bottom: reconstruction of the scourge with two lead balls and a third, grooved cylindrical lead component, alongside the mark it left on the salt-dough. The compatibility between the two impressions is evident.

The distance between the experimental scratches caused by the prototype was slightly different from that detected on the TS, but obviously this problem can be solved by producing fewer grooves in the scourge's cylinder.

Type β and γ scourges for the scratch marks

The marks classified as Type β and γ could have been produced by a scourge equipped with a wooden handle connected to elements capable of scratching the skin without cutting into the underlying flesh.

As a first hypothesis, thin, flexible branches were considered. However, scourges constructed in this way produced marks more than twice the maximum length measured on the TS, so this hypothesis was discarded. For the same reason, the hypothesis of replacing the branches with iron wires, bent at the ends to form small hooks was also discarded, see **(Figure 6)** (all wounds on human skin are involuntary and had no associated health problems, but they are of interest for research).

Figure 6: Example of an impression on a human body from a light strike with a scourge consisting of hooked metal wires connected directly to the handle. The excessive length of the marks produced on the skin is evident.

A better hypothesis involves assuming that these scratches were produced by nails. As a first experiment, four nails, 30 mm in length, were glued with hot glue to four separate cords,

leaving approximately 17 mm of the nail protruding from each cord. These four cords were then tied to a larger cord, which was connected to the scourge's handle. The marks produced proved to be compatible in both shape and dimensions with those present on the TS. It should be noted that sometimes the scratches produced were 3 instead of 4 because some cords overlapped with others.

To produce an analogous scourge using materials available 2000 years ago and of simple construction, four leather cords with a rectangular cross-section of 3 mm by 1 mm were taken. Four wall nails, 30 mm in length, were knotted at the end of each cord, near the nail heads, see **(Figure 7)**. The four cords were connected directly to the wooden handle.

In this case as well, the marks produced by the scourge proved compatible with those on the TS, both in shape and size. It is worth noting that torture structures of this type are easily perishable over time, which is likely why traces of them have been lost today.

Figure 7: Top: an example of a Type β or γ scourge mark on the TS. Bottom: reconstruction of the scourge with nails, each tied with a cord directly to the handle, alongside the mark it left on the saltdough. The compatibility between the two impressions is evident.

Type δ scourges for the rod-like blows marks

For the marks classified as δ, it was hypothesized that a common natural instrument from ancient Rome was used, such as a rod (consider, for instance, the Roman *fasces lictoriae*, composed of a cylindrical bundle of white birch rods bound together by leather straps, in Latin *fasces*), a reed or a branch that was sufficiently flexible yet also strong.

Experimental tests, **(Figure 8)**, in fact demonstrate a similarity in results when using the listed instruments. For this reason, it was decided not to pursue further specific research on the type of scourge for the Type δ marks, simply classifying these marks as rod-like blows.

Figure 8: Experimental marks (bottom) on a human body from Type δ scourges, obtained using rods, reeds or flexible branches. The compatibility of the marks with those visible on the TS (top) is evident.

Concluding Remarks

Since V. Miller's UV photographs of the TS taken in 1978 [31], which better highlight the bloodstains, have recently been made available, the first author deemed it appropriate to update his previous analysis of the scourge wounds based on the visible light photographs taken by Gian Durante in 2000 and 2002.

From this initial analysis, he counted 159 scourge wounds on the frontal image and 213 on the dorsal image, for a total of 372 wounds [30]. This number increased significantly by comparing the scourge marks visible in the detectable light photographs with the corresponding ones taken in UV.

(Table 2) reports the results obtained from this comparison, which can be summarized as follows. The total number of scourge marks was counted as 441, with an uncertainty range of +51/-0, to which an additional uncertainty of ±10 is added, accounting for the subjectivity involved in identifying the scourge marks.

However, given that many scourge marks are not encoded in the TS because it was not in contact with all parts of the wrapped human body, it can be surmised that the scourge wounds inflicted on Jesus' Body could have reached 800 or more. It is immediate to think that such a high number of wounds could have been the triggering pathology of Jesus' death on the cross.

The performed analysis also allowed for the cataloging of bloodstains attributable to different torture instruments and in particular, the following 6 classes of scourge wounds were analyzed in detail: Type α Dumbbell, β Parallel Scratches, γ

Non-parallel Scratches, δ Rod-like Blows, X Unclassifiable Marks and Y Possible Marks.

Since many materials used to construct scourges were relatively perishable over time (for example, leather cords), it is easy to imagine the extreme difficulty of these instruments surviving to the present day and historical documentation confirms this [36].

Consequently, after a detailed measurement of the marks produced by the scourges, reported in **(Table 1)**, the first 3 types of scourges that produced the bloodstains visible on the TS were reconstructed through reverse engineering applied to experimental tests: Type α scourges consisting of multiple cords at the ends of which two lead balls were placed in a dumbbell configuration; Type β and γ scourges consisting of multiple cords to the ends of which nails were knotted; and Type δ scourges consisting of cylindrical rods.

Acknowledgments

The authors thank Dr. Gilbert Lavoie for the permission to use the V. Miller UV photos [31] and G. Durante for the 2000 photos of the TS given to the first author. Thanks also to Andrea Valmorbida who participated in the experimental analysis.

Ethical Statements

The authors, belonging to the Christian Roman Catholic religion, experienced a profound strengthening of faith through scientific studies on the TS.

Conflicts of Interest

The authors declare no conflict of interest.

References

1. Fanti G. New Insights on Blood Evidence from the Turin Shroud Consistent with Jesus Christ's Tortures. Arch Hematol Case Rep Rev 2024;9(1):001-015
2. Fanti G. Holy Fire and Body Image of the Holy Shroud: Divine Photography Hypothesis. World Scientific News WSN 2023;176:104-120.
3. Fanti G. Could an anomaly in Turin Shroud blood reopen the 1988-radiocarbondating result? World Scientific News 2021;162:102-119.
4. Fanti G. A Re-examination of the Pigment-Reinforcement Hypothesis of the Turin Shroud's Bloodstains. World Scientific News 2022;163:99-114.
5. Jumper EJ, Adler AD, Jackson JP, Pellicori SF, Heller JH, Druzik JR. A comprehensive examination of the various stains and images on the Shroud of Turin. Archaeological Chemistry III, ACS Advances in Chemistry 205 1984;22:447-476.
6. Schwalbe LA, Rogers RN. Physics and chemistry of the Shroud of Turin, a summary of the 1978 investigation. Analytical Chemical Acta 1982;135:3-49.
7. Jumper EJ, Mottern RW. Scientific investigation of the Shroud of Turin. Applied Optics 1980;19(12):1909-1912.
8. Mottern RW, London RJ, Morris RA. Radiographic Examination of the Shroud of Turin – a Preliminary Report. Materials Evaluation 1980;38(12):39-44.
9. Morris RA, Schwalbe LA, London JR. X-ray fluorescence investigation of the Shroud of Turin. X-Ray Spectrometry 1980;9(2):40-7.
10. Fanti G. Open issues regarding the Turin Shroud. Scientific Research and Essays 2012;7(29):2507.
11. Fanti G. Hypotheses regarding the formation of the body image on the Turin Shroud. A critical compendium. J Imaging Sci Technol 2011;55(6):060507.
12. Fanti G, Maggiolo R. The Double Superficiality of the Frontal Image of the Turin Shroud. J Opt A: Pure Appl Opt 2004;6:491-503.
13. Garello E. The Shroud and the Popes, Corsi Ed. Turin 1984.
14. Jackson J. The Shroud: A critical summary of data, observations and hypotheses, Turin Shroud Center of Colorado 2017.
15. Fanti G. Byzantine coins influenced by the Shroud of Christ. Jenny Stanford Publishing Pte Ltd. Singapore 2022.
16. Damon PE, Donahue DJ, Gore BH, et al. Radiocarbon dating of the Shroud of Turin. Nature 1989;337:611-615.
17. Rogers RN. Studies on the Radiocarbon Sample from the Shroud of Turin, Thermochimica Acta 2005;425:189-194.
18. McAvoy T. On Radiocarbon Dating of the Shroud of Turin. Int J Archaeol 2021;9(2):34-44.
19. Schwalbe L, Walsh B. On Cleaning Methods and the Raw Radiocarbon Data from the Shroud of Turin. Int J Archaeol 2021;9(1):10-16.
20. Riani M, Atkinson AC, Fanti G, Crosilla F. Regression analysis with partially labelled regressors: carbon dating of the Shroud of Turin. J Statistical Computing 2012.
21. Phillips TJ. Shroud irradiated with neutrons? Nature 1989;337.
22. De Caro L, Barta C, Fanti G, Matricciani E, Sibillano T, Giannini C. Long-Term Temperature Effects on the Natural Linen Aging of the Turin Shroud.
23. Fanti G. Turin Shroud: Medical Impossibility for a Medieval Work of Art. Annal Cas Rep Rev: ACRR-424 2025.
24. Fanti G. Turin Shroud: Comprehensive Impossibility for a Work of Art. Medi Clin Case Rep J 2025;3(1):693-702.
25. Fanti G. The Last Hour of Jesus Christ: A Case Study from Recent New Insights on the Turin Shroud. Medi Clin Case Rep J 2024;2(3):420-422.
26. Fanti G, Ascolese M. Turin Shroud: Etiology of Jesus Christ's Death for Infarction Followed by Hemopericardium. Int Clinc Med Case Rep Jour 2024;3(9):1-12.
27. Fanti G. Shroud of Turin: What Happened to Jesus Christ's Human Body after Death? J Biomed Res Environ Sci 2024;5(10):1278-1287.
28. Fanti G. Turin Shroud: Insights' Review Confirming Biblical Reports About Etiology of Jesus Christ's Death and Resurrection. Medi Clin Case Rep J 2024;2(4):544-556.
29. Fanti G, Gregorek C. Evidence of Jesus' Hematidrosis on the Turin Shroud? Medi. Clin. Rep. Case J., 2025;3(1):741749.
30. Fanti G, Malfi P. The Shroud of Turin - First century After Christ!, Second Edition. Jenny Stanford Publishing Pte. Ltd 2020.
31. Miller V. UV Photos of the Turin Shroud. © Vernon Miller 1978.
32. Vignon P. Le Linceul du Christ. Masson 1902:110-116.
33. Vignon P. Le Saint Suaire de Turin. Masson 1939:55-60.
34. Dictionnaire d'archéologie chrétienne et de liturgie. Letouzey et Ané 1923;5;1640-1642.
35. Faccini B, Scourge Bloodstains on the Turin Shroud: An Evidence for Different Instruments Used, The Shroud of Turin: Perspectives on a Multifaceted Enigma, Ohio Conference 2008.

36. Nicolotti A. The Scourge of Jesus and the Roman Scourge: Historical and Archaeological Evidence. J Study of the Historical Jesus 2017:1-59.